

## Isolation of a novel Anti-KDR3 Single-chain Variable Fragment Antibody from a Phage Display Library

Shirafkan Kordi<sup>1,2</sup>, Mohammad Rahmati-Yamchi<sup>2</sup>, Mehdi Asghari Vostakolaei<sup>3</sup>, Ali Etemadieh<sup>4</sup>  
Abolfazl Barzegari<sup>5</sup>, and Jalal Abdolalizadeh<sup>6,7</sup>

<sup>1</sup>Immunology Research Center, Tabriz University of Medical Sciences, Tabriz, Iran

<sup>2</sup>Department of Medical Biotechnology, Faculty of Advanced Medical Sciences, Tabriz University of Medical Sciences, Tabriz, Iran.

<sup>3</sup>Student Research Committee, Tabriz University of Medical Sciences, Tabriz, Iran

<sup>4</sup>Department of Medical Biotechnology, Tehran University of Medical Sciences, Tehran, Iran

<sup>5</sup>Research Centre for Pharmaceutical Nanotechnology, Tabriz University of Medical Sciences, Tabriz, Iran

<sup>6</sup>Drug Applied Research Center, Tabriz University of Medical Sciences, Tabriz, Iran

<sup>7</sup>Paramedical Faculty, Tabriz University of Medical Sciences, Tabriz, Iran

Received: 29 August 2018; Received in revised form: 5 November 2018; Accepted: 13 November 2018

### ABSTRACT

Vascular endothelial growth factor receptor 2 (VEGFR-2) is known as one of the important antigens playing a vital role in angiogenesis. In this study, phage display technology (PDT) was used to produce a single-chain variable fragment (scFv) antibody against a region of the domain 3 in VEGFR-2 called kinase insert domain receptor 3 (KDR3).

After designing the KDR3 peptide and biopanning, a colony was chosen for scFv antibody expression. Following expression and purification; western blotting, dot blotting and immunofluorescence (IF) were used to evaluate the antibody function. Surface plasmon resonance (SPR) was also employed to measure affinity of produced antibody.

Once a colony was selected and transferred to the expression host, the scFv antibody was expressed in the expected range of 28 kDa. Using a designed chromatography column, antibody purification was found to be about 95%.

In this study, a novel scFv with the capability of binding to KDR3 was isolated and purified and its intracellular function was investigated and verified.

**Keywords:** Monoclonal antibody; Kinase insert domain receptor (KDR) 3 Phage display; Single-chain variable fragment (scFv); Vascular endothelial growth factor receptor-2 (VEGFR2)

### INTRODUCTION

Angiogenesis refers to the formation of new blood vessels from pre-existing ones. This phenomenon is

a naturally occurring multi-stage process although can be seen in pathophysiological conditions. Angiogenesis is also a procedure required for invasion, metastasis, and cancer progression. In this respect, the vascular,

---

**Corresponding Author:** Jalal Abdolalizadeh, PhD;  
Clinical Biochemistry, Drug Applied Research Center, Tabriz

---

University of Medical Sciences, Tabriz, Iran. Tel/Fax: (+98 41) 33371971, E-mail: jabdolalizadeh@gmail.com

Ser264, Ser265, and Lys266.<sup>13</sup> endothelial growth factor (VEGF) is known as a key factor in the proliferation and migration of endothelial cells, which is the basis of new vein formation.<sup>1,2</sup> The biological action of this VEGF is applied to target cells by interacting with tyrosine kinase receptors on the cell plasma membrane. These receptors, after binding to their ligand, become dimers and are auto phosphorylated, eventually inducing an intracellular cascade of events. Known tyrosine kinase receptors associated with these growth factors are VEGFR-1, VEGFR-2, VEGFR-3, and Neuropilins.<sup>3,4</sup> The VEGFA is a major factor in angiogenesis and acts through activating VEGFR-1 and VEGFR-2 receptors.<sup>5</sup> There is also a consensus that the VEGF and its most important receptor, the VEGFR-2, are the main regulators of angiogenesis.<sup>6</sup> VEGF signaling and its intracellular cascade results to angiogenesis in the tumor similarly stimulates rapid growth of the tumor and facilitates metastasis.<sup>7</sup> Therefore, preventing this cascade can result in anti-angiogenic and anti-tumor response.<sup>8</sup> Several monoclonal antibodies have been further produced against the VEGF or the VEGFR, which prevent or significantly reduce angiogenesis.

Human antibodies are more preferred than murine and chimeric antibodies because they induce low immunogenicity in their hosts. One of the methods for producing fully human antibodies is the phage display technology (PDT), which was first introduced by Smith in 1985.<sup>9</sup> The PDT can be used to produce phage libraries expressing a single-chain variable fragment (scFv) antibody. These libraries with their high diversity can help in the production of high-affinity antibodies against almost all antigens. The scFv antibody against the KDR3 can be also produced using the PDT. The scFv antibody fragments are classified as the fourth generation of antibodies and they are fully humanized, so they have been used in clinic without the immunogenicity concerns. In pharmacokinetic insight, the blood clearance of scFv as an important issue, is favorable. Due to the elimination of Fc receptor in this kind of antibody, utilization of scFv results in low non-specific binding to the Fc receptors that expressed on the normal cells.<sup>10</sup> The scFv fragments show high penetration in tumor cells and tissues which is related to their small size and low molecular weight. Easiness in large scale production of scFv and no need to animals for this process introduce scFv as a strong agent for clinical and laboratory applications.<sup>11</sup>

The extracellular fragment of kinase insert domain receptor 3 (KDR3) is composed of seven immunoglobulin-like domains. There is also a tyrosine kinase domain located in the intracellular side. Among the seven extracellular domains with 1356 amino acids, it has been shown that domains 1-3, especially domain 3, are sufficient and necessary for high affinity binding with VEGF.<sup>12-14</sup> It has been also shown that the domain 3 has two different sets of amino acids playing a vital role in antibody binding to the receptor, one of Ile256, Asp257, Glu261, Leu313, and Thr315, and another of Tyr262, Pro263

The purpose of this study was to isolate mAb against a peptide, designed from a fragment of KDR3 using PDT.

## MATERIALS AND METHODS

### Designing of KDR3 Peptide for Selection Phase

Various characteristics of the KDR3 peptide were studied as antigens including epitope, antigenicity, and especially the accessibility domains, using the online database of IEDB Analysis Resource<sup>15</sup> to identify regions of this target protein that can be employed to prepare antibodies via PDT. The Ethics Committee of Tabriz University of Medical Sciences approved the research project (N. 94.2- 1.8).

### Selection of scFv by Biopanning

After dissolving the KDR3 peptide in a carbonate buffer at pH 8.5, 100 µL was added to the wells of 96-well plates and incubated overnight at 4°C. The biopanning procedure for antibody selection was performed as previously described.<sup>16,17</sup> Polyclonal and monoclonal phage ELISA were also used to verify the ability of scFv expression.

### Homology Modeling, Assessment and Docking

Using automodel.very\_fast method in Modeller v9.18, Modeller was performed to get an approximate model very quickly. Four scFv sequences (A9K, F12K, G12K, and H6K) were also used as input in automodel.very\_fast method. Initially, BlastP was performed against the given sequences and three templates were found for each sequence. Then a multiple sequence alignment was produced using Clustal Omega. Automodel.very\_fast method in Modeller created a model for each sequence. To end with, ClusPro docking server<sup>18</sup> was used for binding

affinity calculation of each predicted model with KDR3. The best models were used in Modeller v9.18 software for performing HM via the crystal structures of 5GRW-A, 5gs1-C, and 5GS3-H as the templates. Modeller v9.18 software was also applied for performing HM using the crystal structures of 5GRW-A, 5gs1-C and 5GS3-H as the templates. As mentioned above, BlastP was performed against the given sequence and three templates were found, which had been used as inputs for multiple sequence alignment via Clustal Omega.

For further analyses, among 10000 generated models, 10 top models were chosen based on their molecular pdf (molpdf) score, GA341 score, DOPE score, normalized dope score, as well as DOPEHR score. The refinement and energy minimizing of the selected model was further carried out using GalaxyRefine<sup>19</sup> and NOMAD-REF<sup>20</sup> servers. VADAR (Volume, Area, Dihedral Angle Reporter) server<sup>21</sup> and ProSA<sup>22</sup> were also applied for evaluation of the quality of the homology model and assessment of the accuracy and reliability of the modelled structures. TM-align web tool<sup>23</sup> was then performed to compare the resulted 3D model of A9K with the best template structure (Chain H from PDB ID: 5GS3). A9K-KDR3 (PDB:3V2R chain R) binding affinity and docking score were similarly assessed using both ClusPro docking and HADDOCK servers.<sup>24</sup>

### Expression and Extraction of scFv in the Bacterial Expression System

In order to express the selective scFv (A9K), the phage derived from colony A9K was added to host *E. coli* (HB2151 strain). The expression and extraction of scFv were also performed as previously described.<sup>16,17</sup>

### Purification of scFv by Affinity Chromatography using Protein A Sepharose 4B

Anti-KDR3 scFv antibody fragments were purified by affinity chromatography using protein A Sepharose 4B.<sup>25</sup> Briefly, 5 mL of protein A-Sepharose 4B column (Amersham Biosciences, Freiburg, Germany) was packed and then equilibrated with the binding buffer (1x PBS, pH 7.4). The mixture of the secreted scFv and periplasmic fractions were then applied to the column at a flow rate of 50 cm/h. Afterwards; the column was washed via washing buffer with five column volumes and finally scFvs were eluted with elution buffer (0.1M Glycine-HCl, pH 2.7) under isocratic conditions. The

fractions containing antibody fragments were pooled and the pH was adjusted to 7.5 by 2 M Tris-HCl, pH 8.0. Fractions were also assessed by sodium dodecylsulfate-polyacrylamide gel electrophoresis (SDS-PAGE) and the pure fractions were collected. The samples were dialyzed overnight against 1x PBS and the final products were quantified using a UV spectrophotometer at optical density (OD) of 280 nm.

### SDS-PAGE and Western Blot Analysis

To evaluate the size and purity of the scFv fragments, the products were electrophoresed on a 12% SDS-PAGE. The bands were then visualized after Coomassie Blue-R250 staining.

The western blot was also designed to confirm the function of purified scFv. For this purpose, after electrophoresis, the products were transferred to a polyvinylidene fluoride (PVDF) membrane (Millipore, Billerica, MA, USA) using a semidry transfer device (Amersham Biosciences, Freiburg, Germany). After blocking the PVDF membrane with 5% skim milk, the primary antibody of mouse anti-myc antibody (Santa Cruz Biotechnology, Santa Cruz, CA, USA) was added with the ratio of 1 to 1000. After washing with TBST, the secondary antibody of the HRP-conjugated anti-mouse IgG (Santa Cruz Biotechnology, Santa Cruz, CA, USA) was applied with the ratio of 1 to 2500. Then, the membrane was rewashed and the enhanced chemiluminescence (ECL) substrate (Amersham Biosciences, Freiburg, Germany) was added immediately to observe the bands.

### Dot Blotting Analysis

To test the specificity and cross-reactivity of the obtained scFvs, a dot blotting test was employed. Bovine serum albumin (BSA) and KDR3 peptide were blotted onto PVDF. Then, the membrane was blocked and incubated with scFv. After washing, the membrane was incubated with mouse anti-myc antibody and subsequently with HRP-conjugated anti-mouse IgG. The ECL substrate was also used for the visualization of protein bands.

### Evaluating the Binding Affinity of scFv

The SPR method with a multi-parameter SPR device (MP-SPR Navi 210A, BioNavis Ltd, Finland) was used to study the purified scFv kinetic properties and to evaluate its binding affinity to the extracellular KDR3 protein (KDR3 peptide).<sup>26</sup>

First, gold chip was placed at RT in the presence of 5mM MUA (11-mercaptoundecanoic acid) in ethanol and Milli-Q-water, respectively, at a ratio of 7 to 3. After 24 hours, the chip was washed several times with PBS buffer and ethanol.<sup>27</sup> The MUA-sensor was then placed in the SPR instrument. The device started to work by passing the PBS buffer. Next, the sensor surface was washed with NaCl (2 M) and NaOH (0.1 M). To activate the chip surface, the EDC (0.2 M) and NHS (0.05 M) solutions were injected at a ratio of 1 to 1. Immediately after activation, the scFv solution was injected in the PBS buffer with a flow rate of 10 $\mu$ l/min for 8 min on a part of the slide surface. The other part of the slide without scFv was introduced as a negative control to the device. The ethanolamine-HCl (1.0 M) blocker solution; and then, serial concentrations of KDR3 peptide were added to the chip in the PBS buffer. Finally, the kinetic properties of affinity and dissociation were analyzed using the SPR NaviTM Data Viewer software.

### IF Microscopy

Human Umbilical Vein Endothelial Cells (HUVEC) were cultured in RPMI 1640 medium (Flow Laboratories, Opera, Italy) containing 10% FBS. The plate was incubated with confluence about 70% overnight with 5% CO<sub>2</sub> at 37°C. After washing, the

plate was blocked by blocker solution which was followed by addition of 10  $\mu$ g/mL of the produced scFv to the cells. After washing the cells, FITC-labeled goat anti-mouse IgG was added and incubated for 1 hour in RT. After final washing and adding 90% glycerol, the cells were examined under a fluorescence microscope.

## RESULTS

### Peptide Design from KDR3

Beside the IEDB online database, further investigation into the biochemical structure of the KDR3 protein by the VMD 1.9.2 software determined that the 15-aa peptide with the sequence of -COOH PSSHHQHKKLVNRDL NH<sub>2</sub>- could be used.

This fragment synthesized by Mimotopes Co. (Australia) chemically with 95% purification, was called KDR3 peptide. The peptide was also evaluated and verified by mass spectrophotometry and HPLC. The availability of the fragment selected as the target, which was obtained by the IEDB Analysis Resource was shown in Figure 1.

According to the scores of this database, the amino acids which were above the threshold line on the graph were fully available on the protein surface. Other features including Epitope and Antigenicity could be reviewed by this database.

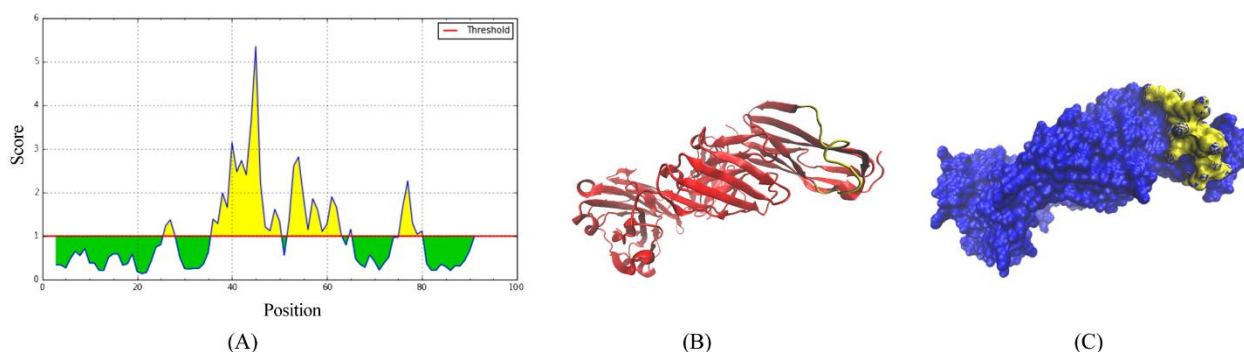


**Figure 1.** (A) Analysis of the human Kinase insert domain receptor (KDR) 3 amino acid sequences using Bepipred linear epitope prediction in Immune Epitope Database (IEDB). The residues which can participate in the epitope structures have positive scores (yellow) and negative scores for other residues (green). A linear continues peptide with 15 residues, i.e. PSSHHQHKKLVNRDL from the 263 to 277 residues could be a target for antibodies. The position of this target peptide in the secondary (B) and three-dimensional structure (C) of the human KDR3 virtualized using visual molecular dynamics (VMD) 1.9.1 software (yellow).

## Isolation of Anti-KDR3 Single-chain Antibody

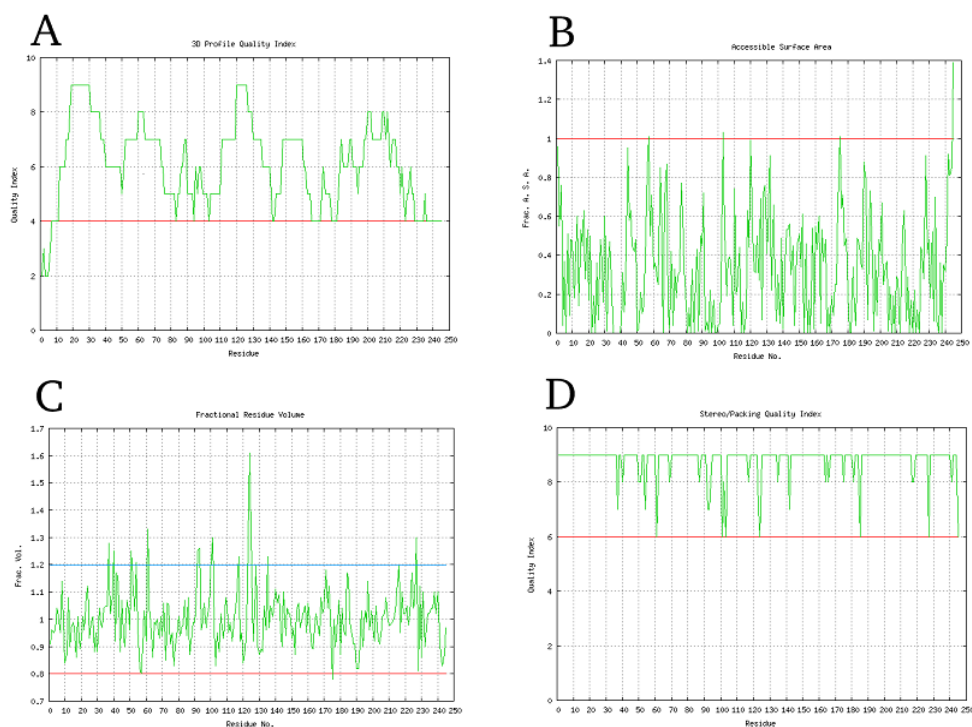


**Figure 2.** Quality assessment of the best model using (Volume, Area, Dihedral Angle Reporter) VADAR. A) 3D profile quality index, showing good local environment, packing and hydrophobic energy B) Accessible surface area, showing the visible surface area of the residue that a water molecule could touch C) Fractional residue volume and D) Stereo/Packing quality index, showing specific "problem" residues with score less than 6.

### Modeling, Assessment, and Docking

The best results were selected for all docked models based on the lowest calculated energy ( $E=0.50E_{rep}+0.20E_{att}+600E_{elec}+0.25E_{DARS}$ ); which were -337.0, -294.5, -315.6 and -333.7 for A9K, F12K, G12K, and H6K, respectively. Quality assessment of the best model was also checked using VADAR (Figure 2). Compared with experimentally-validated protein structures (Figure 2A), the total model quality calculated by ProSA Z-score was -7.66 implicating a very high quality of the model. ProSA web tool (Figure 2B) confirmed the local model quality. Accuracy of HM prediction method assessed based on TM-score of A9K-5GS3-H structural alignment was equal to 0.83 (Figure 3).

### Evaluating the Expression of Antibody Fragments

The phage obtained from the A9K clone, which was found to be a proper clone for continued testing after sequencing and docking, was transferred to the HB2151 strain of host *E. coli*. After its induction by Isopropyl-beta-D-thiogalactopyranoside (IPTG), scFvs

were also extracted from the periplasmic and cytoplasmic regions and electrophoresed by 12% SDS-PAGE. The protein bands were observed using the Coomassie Brilliant Blue staining.

The extracted scFvs shown in Figure 4 were within the expected weight range (approximately 28 kDa) and the expressions were obvious at different times of induction.

### Western Blotting and Dot Blotting of Purified scFv

A9K scFv was resolved by 12% SDS-PAGE under reducing conditions. Then, western blotting analysis was done using anti-Myc and HRP conjugated anti-mouse antibodies. ECL substrate was used for the visualization of protein bands. As a result, Figure 5A and Figure 5B represented SDS-PAGE and western blot analysis of purified scFv with a 28 kDa molecular weight. By the ImageJ software, antibody purification was estimated to be about 95%. Dot blotting analysis showed specific binding of purified scFv to KDR3 peptide with no cross-reactivity with BSA (Figure 5C).

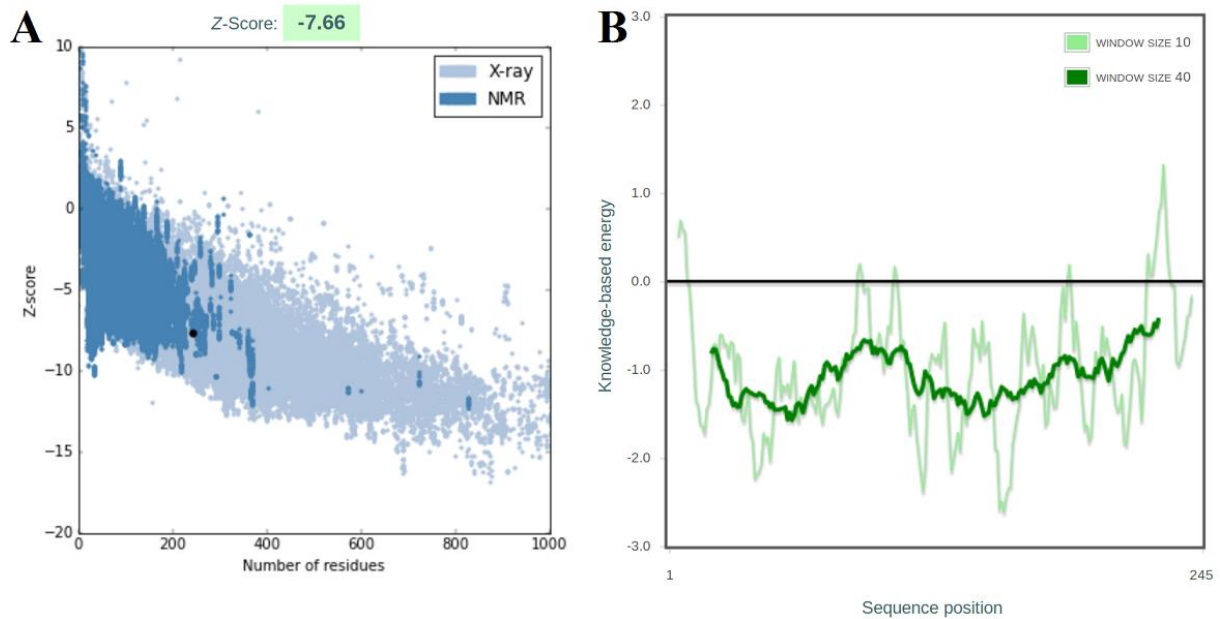


**Figure 3.** A) ProSA Z-score plot of modeled 3D structure of A9K. The bold black circle shows the position of this model among experimentally solved protein structures, which means that our predicted model is in the range of experimentally solved structures. B) Sequence position model quality. The more negative are indicative of the greater accuracy.

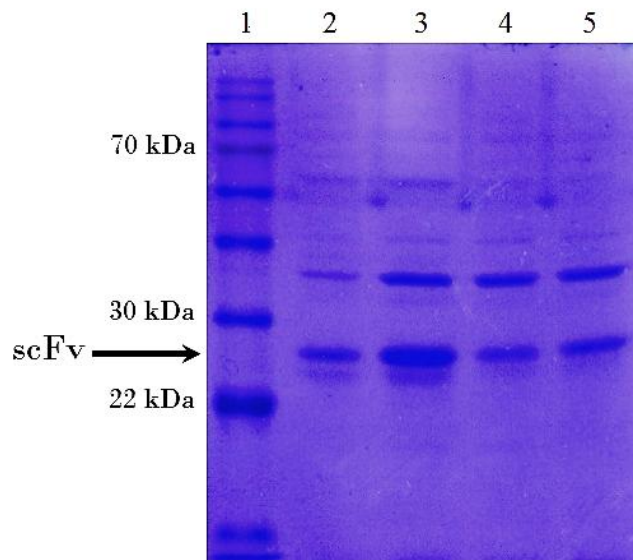


**Figure 4.** The electrophoresis of single-chain variable fragment (scFv) expressed from periplasmic and cytoplasmic fractions. The expression of scFv is due to induction of *E. coli* strain HB2151 by 0.2 mM of isopropyl  $\beta$ -D-thiogalactopyranoside (IPTG) at different times. After extraction, each fraction was electrophoresed on 12% sodium dodecylsulfate-polyacrylamide gel electrophoresis (SDS-PAGE) and stained with Coomassie Brilliant Blue. The Lane1: ladder, Lane2: the product of scFv expressed in the cytoplasmic fraction at 6 h after induction, and Lane 3, 4 and 5: the product of scFv expressed in the periplasmic fraction at 11, 9 and 6 h after induction, respectively.

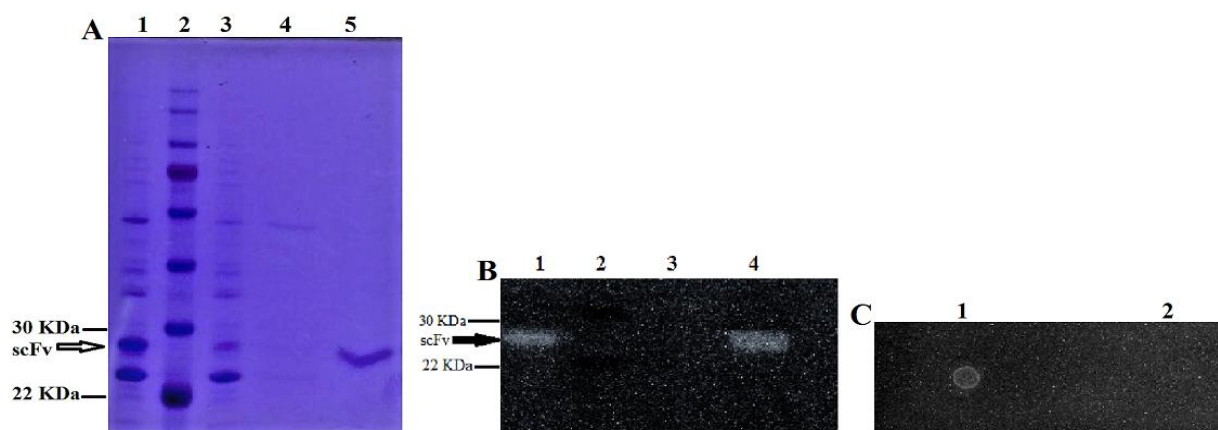


**Figure 5.** Binding analysis of the purified scFv to KDR3 peptide using western blot and dot blot assay. A) Electrophoresis of purified scFv against KDR3. The lanes are respectively 1- purified scFv from cytoplasmic fraction 2- ladder 3- purified scFv from the periplasmic fraction 4- wash from the periplasmic fraction and 5- elution from the periplasmic fraction. B) Binding analysis of the purified scFv to KDR3 peptide using Western blot. The lanes are respectively 1- elution from the cytoplasmic fraction 2- ladder fraction 3- wash from the periplasmic fraction and 4- elution from the periplasmic. C) Binding analysis of the purified scFv to KDR3 peptide by dot blot assay. Line 1 show a specific binding of purified scFv to KDR3 peptide and line 2 no cross-reactivity to BSA, respectively. KDR3: Kinase insert domain receptor, scFv: single-chain variable fragment

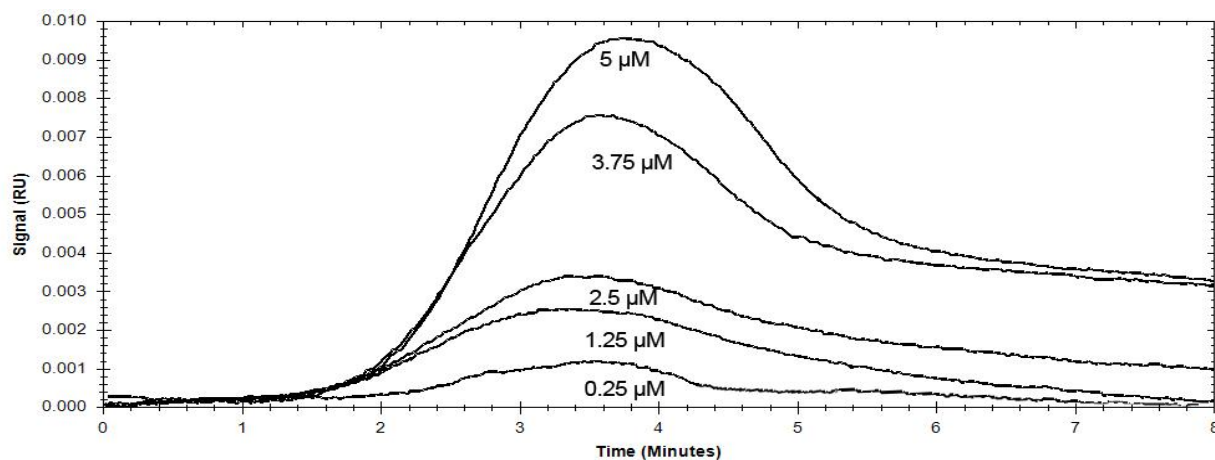


**Figure 6.** Surface plasmon resonance (SPR) analysis of the purified A9 single-chain variable fragment (scFv). The scFv immobilized on a mercaptoundecanoic acid (MUA)-modified Au-sensor slide at pH 4.5 by amine coupling protocol. The response unit (RU) of the scFv was approximately 3.6 times more than that of blank channel and Kinetic parameters after injection of different concentrations of the peptide shown the scFv had  $KD=8.69 \times 10^{-7}$  M.

### Investigation into Kinetic Properties of scFv Using SPR

Figure 6 showed the dose-response sensograms of the reaction between the scFv stabilized on the chip surface and different concentrations of peptide from 0.25 to 5 μM. The results of affinity ( $K_a$ ) and

dissociation ( $K_d$ ) of different concentrations of KDR3 peptide were also analyzed by the software and the affinity constant ( $KD$ ) was calculated based on these results. These data indicated that  $K_a$  was  $6.1 \times 10^3 \text{ M}^{-1} \text{ s}^{-1}$  and  $K_d$  was  $5.31 \times 10^{-3} \text{ s}^{-1}$ . The affinity limit of scFv range was within nM ( $KD= 8.69 \times 10^{-7}$  M).

### IF Analyses

To evaluate the cellular function of scFv A9K, it's binding to HUVECs, cultured and fixed in the plate,

were examined using a fluorescence microscope. The selected specific scFvs binding with the cells were shown in Figure 7.

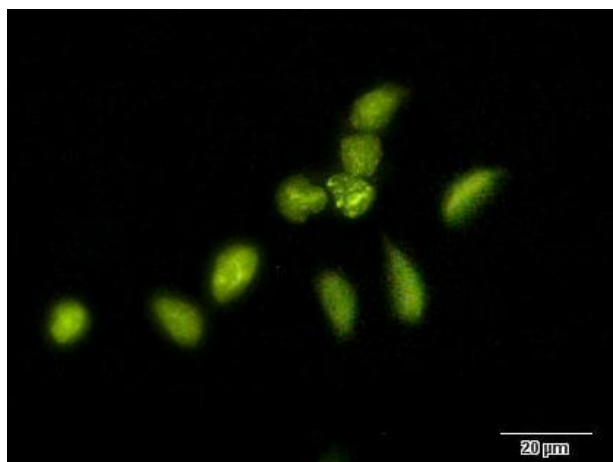


**Figure 7. Fluorescence microscopy of Human Umbilical Vein Endothelial Cells (HUVECs) treated with scFv A9K. After adding mouse anti-myc antibody and adding Fluorescein isothiocyanate (FITC)-labeled goat anti-mouse IgG secondary antibody and final wash, 90% glycerol was added to the cells and observed under fluorescence microscope.**

### DISCUSSION

Monoclonal antibodies can detect and inhibit cancer cells through binding to specific antigens on the cell surface.<sup>28</sup> The success of this method depends, to a large extent, on finding an ideal antigen for cancer cell targeting. In this respect, the KDR3 is known as one of the key antigens on the cancer cell surface, playing a role in the angiogenesis. Therefore, the prevention of angiogenesis by linking the scFv to the KDR3 can prevent cancer growth or metastasis. This does not happen sometimes because angiogenesis is regulated by multiple pathways and by blocking a path (VEGFR-2 / VEGF), other pathways may be activated and angiogenesis occurs.<sup>6</sup> In one of these ways, the produced scFv can be linked to the core shell of the nanoparticles carrying therapeutic drugs and to overcome this problem, it is released to be specifically linked to KDR3. This function not only reduces the process of angiogenesis, but also leads to the release of nanoparticle contents on cancer cells and destroys them. Today, there is a growing trend in targeted therapy with nanoparticles.<sup>29,30</sup> Several studies have also shown that the most important fragments of KDR3 for antibody production are the first to the third domains, especially the third domain.<sup>12,13</sup> In the light of previous studies, a segment of the KDR3 was also selected with regard to its accessibility and design for

peptide synthesis. Biopanning steps were also repeated four times, usually three to four steps.

The expression level of the selected scFv in the bacterial expression vector had a proper effect. This level of expression might be due to the use of an appropriate phagemid vector, which could be found in this type of library. These manipulated phagemid vectors were capable of penetrating the bacteria, for easy cloning and rapid proliferation.<sup>16,31</sup>

The scFvs could be extracted from both the periplasmic and cytoplasmic spaces using the correct extraction method. In the periplasmic space, the protein could have the correct folding and high sustainability.<sup>32</sup>

In this study, the production of scFv was optimized. There are many factors involved in protein production,<sup>33</sup> namely time, IPTG level, ampicillin, temperature, and bacterial growth OD in the present study. In the literatures, the induction by IPTG were considered at in the middle of the growth phase i.e. OD 0.6 but it could be done at the end of the growth phase and even the stationary phase i.e. ODs higher than 0.6.<sup>33,34</sup> The results of this study showed that the highest scFv expression was related to the time, about 11 hours after induction with IPTG in OD of 1.7. Moreover, the best values for other items included IPTG of 0.2mM, temperature of 28°C and 50 μg/mL of ampicillin to achieve maximum scFv expression. In other studies, reported that used 0.2-1 mM IPTG and



25-30°C temperature.<sup>31-36</sup>

Affinity chromatography with a stabilized biomolecule, such as protein A, had a high potential for absorbing antibodies. It was found that the efficiency of this purification method was high, but it was uneconomical due to the costly nature of these columns at the industrial scale.

Analyzing the purity of antibodies by observing the bands formed in SDS-PAGE revealed purification with a high yield of about 90%. The yield of antibody in this one-step purification method was more significant than the yield in other purification methods.<sup>37</sup> The western blot method was also used to verify the expression. The western blotting and dot blotting techniques confirmed the purified scFv function.

Biosensor tests, including SPR, are capable of accurately measuring the signals from ligand-receptor or antigen-antibody binding, and recording their activity at the molecular level. These experiments are quite quantitative and feasible for samples with a low amount and in the least time with high sensitivity. By analyzing the purified scFv binding affinity when comparing them with other antibodies, it was found that the given antibody had acceptable binding affinity. In the studies that scFv fragments have been used to the cell surface receptors as targets, the binding affinity were in line with the results of this study. Whereas, binding affinity in the studies that used scFv to target VEGFR-2 were in the range of nano and picomolar in unit. However, the high binding affinity of an antibody is not responsible for its better efficacy.<sup>38</sup>

The results of fluorescence microscopy demonstrated that the isolated scFv was linked to the KDR3 cell surface, indicating the proper functioning of the scFv. The fluorescence signal in these cells was slightly lower than what was expected, probably because when the scFv was bound to the receptor (KDR3) on the living cell surface, a large number of them could enter into the cell by endocytosis. In the final stages, when the conjugated antibody was added, the amount of scFv linked to the KDR3 will could decrease on the cell surface, thereby reducing the fluorescence signal. To address this problem, the cells were required to be fixed from the beginning, or the primary FITC scFv was needed to be used in a single step.

We isolated and purified an anti-human KDR3 scFv fragment by using of PDT. Since the functionality of the isolated scFv was confirmed using three criteria i.e.

in silico docking, SPR and IF, it would be used to detect KDR3 as an effective target in the human cancers. However, to use this scFv in cancer immunotherapy, we shall focus on affinity maturation and in vivo models using computational design/protein engineering and animal models.

In this study, a novel scFv capable of binding KDR3 was isolated and purified, and its function was investigated and verified on the cell surface.

At present, it is possible to label the scFv with radioactive or fluorescence materials for application in detection methods, both in vitro and in vivo. In general, it is hoped to enhance the effectiveness of antibodies in future investigations in all settings used for therapeutic, diagnostic and imaging purposes.

### ACKNOWLEDGEMENTS

These data are part of PhD thesis registered in Tabriz University of Medical Sciences, Iran. The authors are grateful for financial support by the Immunology Research Center of Tabriz University of Medical Sciences.

### REFERENCES

1. Hsu JY, Wakelee HA. Monoclonal antibodies targeting vascular endothelial growth factor. *BioDrugs* 2009; 23(5):289-304.
2. Suto K, Yamazaki Y, Morita T, Mizuno H. Crystal Structures of Novel Vascular Endothelial Growth Factors (VEGF) from Snake Venoms: insight into selective VEGF binding to kinase insert domain-containing receptor but not to fms-like tyrosine kinase-1. *J Biol Chem* 2005; 280(3):2126-31.
3. Gupta K, Zhang J. Angiogenesis: a curse or cure? *Postgrad Med J* 2005; 81(954):236-42.
4. Otrrock ZK, Makarem JA, Shamseddine AI. Vascular endothelial growth factor family of ligands and receptors: review. *Blood Cells Mol Dis* 2007; 38(3):258-68.
5. Shibuya M, Claesson-Welsh L. Signal transduction by VEGF receptors in regulation of angiogenesis and lymphangiogenesis. *Exp Cell Res* 2006; 312(5):549-60.
6. Zhao Y, Adjei AA. Targeting angiogenesis in cancer therapy: moving beyond vascular endothelial growth factor. *Oncologist* 2015; 20(6):660-73.
7. Hicklin DJ, Ellis LM. Role of the vascular endothelial growth factor pathway in tumor growth and angiogenesis. *J Clin Oncol* 2005; 23(5):1011-27.

8. Carmeliet P, Jain RK. Molecular mechanisms and clinical applications of angiogenesis. *Nature* 2011; 473(7347):298-307.
9. McCafferty J, Griffiths AD, Winter G, Chiswell DJ. Phage antibodies: filamentous phage displaying antibody variable domains. *Nature* 1990; 348(6301):552.
10. Wong KJ, Baidoo KE, Nayak TK, Garmestani K, Brechbiel MW, Milenic DE. In vitro and in vivo pre-clinical analysis of a F (ab')<sub>2</sub> fragment of panitumumab for molecular imaging and therapy of HER1-positive cancers. *EJNMMI Res* 2011; 1(1):1.
11. Mukai Y, Okamoto T, Kawamura M, Shibata H, Sugita T, Imai S, et al. Optimization of anti-tumor necrosis factor- $\alpha$  single chain Fv displayed on phages for creation of functional antibodies. *Pharmazie* 2006; 61(10):889-90.
12. Fuh G, Li B, Crowley C, Cunningham B, Wells JA. Requirements for binding and signaling of the kinase domain receptor for vascular endothelial growth factor. *J Biol Chem* 1998; 273(18):11197-204.
13. Lu D, Kussie P, Pytowski B, Persaud K, Bohlen P, Witte L, et al. Identification of the residues in the extracellular region of KDR important for interaction with vascular endothelial growth factor and neutralizing anti-KDR antibodies. *J Biol Chem* 2000; 275(19):14321-30.
14. Kordi S, Rahmati-Yamchi M, Vostakolaei MA, Barzegari A, Abdolalizadeh J. Purification of a Novel Anti-VEGFR2 Single Chain Antibody Fragment and Evaluation of Binding Affinity by Surface Plasmon Resonance. *Adv Pharm Bull* 2019; 9(1):64-9.
15. Larsen JEP, Lund O, Nielsen M. Improved method for predicting linear B-cell epitopes. *Immunome Res* 2006; 2(1):2.
16. Abdolalizadeh J, Nouri M, Zolbanin JM, Baradaran B, Barzegari A, Omid Y. Downstream characterization of anti-TNF- $\alpha$  single chain variable fragment antibodies. *Hum Antibodies* 2012; 21(1-2):41-8.
17. Abdolalizadeh J, Nouri M, Zolbanin JM, Barzegari A, Baradaran B, Barar J, et al. Targeting cytokines: Production and characterization of anti-TNF- $\alpha$  scfvs by phage display technology. *Curr Pharm Des* 2013; 19(15):2839-47.
18. Kozakov D, Hall DR, Xia B, Porter KA, Padhorny D, Yueh C, et al. The ClusPro web server for protein-protein docking. *Nat Protoc* 2017; 12(2):255-78.
19. Heo L, Park H, Seok C. GalaxyRefine: protein structure refinement driven by side-chain repacking. *Nucleic Acids Res* 2013; 41(W1):W384-W8.
20. Lindahl E, Azuara C, Koehl P, Delarue M. NOMAD-Ref: visualization, deformation and refinement of macromolecular structures based on all-atom normal mode analysis. *Nucleic Acids Res* 2006; 34(suppl\_2):W52-W6.
21. Willard L, Ranjan A, Zhang H, Monzavi H, Boyko RF, Sykes BD, et al. VADAR: a web server for quantitative evaluation of protein structure quality. *Nucleic Acids Res* 2003; 31(13):3316-9.
22. Wiederstein M, Sippl MJ. ProSA-web: interactive web service for the recognition of errors in three-dimensional structures of proteins. *Nucleic Acids Res* 2007; 35(suppl\_2):W407-W10.
23. Zhang Y, Skolnick J. TM-align: a protein structure alignment algorithm based on the TM-score. *Nucleic Acids Res* 2005; 33(7):2302-9.
24. Dominguez C, Boelens R, Bonvin AM. HADDOCK: a protein-protein docking approach based on biochemical or biophysical information. *J Am Chem Soc* 2003; 125(7):1731-7.
25. Abdolalizadeh J, Nouri M, Zolbanin JM, Baradaran B, Barzegari A, Omid Y. Downstream characterization of anti-TNF- $\alpha$  single chain variable fragment antibodies. *Hum Antibodies* 2012; 21(1-2):41-8.
26. Sharifi M, Dolatabadi JEN, Fathi F, Rashidi M, Jafari B, Tajalli H, et al. Kinetic and thermodynamic study of bovine serum albumin interaction with rifampicin using surface plasmon resonance and molecular docking methods. *J Biomed Opt* 2017; 22(3):037002.
27. Fathi F, Rezabakhsh A, Rahbarghazi R, Rashidi M-R. Early-stage detection of VE-cadherin during endothelial differentiation of human mesenchymal stem cells using SPR biosensor. *Biosens Bioelectron* 2017; 96:358-66.
28. Fasihi-Ramandi M, Amani J, Salmanian A, Moazzeni S, Ahmadi K. Production and characterization of new anti-human CD20 monoclonal antibody. *Iran J Allergy Asthma Immunol* 2015; 14(5):502-8.
29. Kordi S, Zarghami N, Akbarzadeh A, Rahmati YM, Ghasemali S, Barkhordari A, et al. A comparison of the inhibitory effect of nano-encapsulated helenalin and free helenalin on telomerase gene expression in the breast cancer cell line, by real-time PCR. *Artif Cells Nanomed Biotechnol* 2016; 44(2):695-703.
30. Mousavi SA, Ghotaslou R, Kordi S, Khoramdel A, Aeenfar A, Kahjough ST, et al. Antibacterial and antifungal effects of chitosan nanoparticles on tissue conditioners of complete dentures. *Int J Biol Macromol* 2018; 118:881-5.
31. Akbari B, Farajnia S, Zarghami N, Mahdih N, Rahmati M, Khosroshahi SA, et al. Design, expression and evaluation of a novel humanized single chain antibody

- against epidermal growth factor receptor (EGFR). *Protein Expr Purif* 2016; 127:8-15.
32. Xi H, Yuan R, Chen X, Gu T, Cheng Y, Li Z, et al. Purification and on-column refolding of a single-chain antibody fragment against rabies virus glycoprotein expressed in *Escherichia coli*. *Protein Expr Purif* 2016; 126:26-32.
  33. Mesgari-Shadi A, Sarrafzadeh MH. Osmotic conditions could promote scFv antibody production in the *Escherichia coli* HB2151. *BioImpacts* 2017; 7(3):199-206.
  34. Rahbarnia L, Farajnia S, Babaei H, Majidi J, Dariushnejad H, Hosseini MK. Isolation and characterization of a novel human scFv inhibiting EGFR vIII expressing cancers. *Immunol Lett* 2016; 180:31-8.
  35. Vostakolaei MA, Molavi O, Hejazi MS, Kordi S, Rahmati S, Barzegari A, et al. Isolation and characterization of a novel scFv antibody fragments specific for Hsp70 as a tumor biomarker. *Journal of cellular biochemistry*. 2019.
  36. Aghebati-Maleki L, Younesi V, Baradaran B, Abdolalizadeh J, Motallebnezhad M, Nickho H, et al. Antiproliferative and apoptotic effects of novel anti-ROR1 single-chain antibodies in hematological malignancies. *SLAS Discov* 2017; 22(4):408-17.
  37. Akbari B, Farajnia S, Zarghami N, Mahdih N, Rahmati M, Khosroshahi SA, et al. Construction, expression, and activity of a novel immunotoxin comprising a humanized antiepidermal growth factor receptor scFv and modified *Pseudomonas aeruginosa* exotoxin A. *Anticancer Drugs* 2017; 28(3):263-70.
  38. Zhang J, Li H, Wang X, Qi H, Miao X, Zhang T, et al. Phage-derived fully human antibody scFv fragment directed against human vascular endothelial growth factor receptor 2 blocked its interaction with VEGF. *Biotechnol Prog* 2012; 28(4):981-9.